

Fabrication of nanoscale photochromic materials by vapor deposition method

Arnaud Spangenberg,¹ Arnaud Brosseau,¹ Rémi Metivier,¹ Michel Sliwa,^{1†} Keitaro Nakatani,^{1*} Tsuyoshi Asahi² and Takayuki Uwada²

¹PPSM, ENS Cachan, CNRS, UniverSud, 61 av President Wilson, F-94230 Cachan, France

²Department of Applied Physics, Osaka University, Yamadaoka 2-1, Suita, Osaka 565-0871, Japan

Received 7 February 2007; revised 27 April 2007; accepted 11 May 2007

ABSTRACT: Vapor deposition method was used to obtain nanocrystals of *N*-(3,5-di-*tert*-butylsalicylidene)-4-aminopyridine (**1**) and *N*-(3,5-di-*tert*-butylsalicylidene)-4-iodoaniline (**2**), and nanoscale thin layers (65 nm thick) of *cis*-1,2-dicyano-1,2-bis(2,4,5-trimethyl-3-thienyl)ethene (**3**). Compound **3** was also deposited on a substrate previously covered by gold nanoparticles ($\varnothing = 100$ nm). Nanoscale crystals of **1** and **2** showed similarities with bulk crystals: they exhibit photochromic properties and they have similar shapes according to Atomic force microscopy (AFM) investigations. The thin layers of **3**, with and without gold nanoparticles, showed light-induced absorption change in the visible. Copyright © 2007 John Wiley & Sons, Ltd.

KEYWORDS: photochromism; hybrid materials; nanomaterials; vapor deposition; gold nanoparticles

INTRODUCTION

Light-induced color changes in organic compounds have been discovered more than a century ago.¹ Despite such an old history, many research groups are still actively working on this phenomenon, called photochromism.² This category of molecules has been used in daily life as switchable devices, for example in variable transmittance lenses.³ In the 21st century, other applications are targeted (e.g., in information technology), based on the fact that switching occurs at a molecular scale (Scheme 1).⁴ Indeed, if addressing individual molecules is possible, it can be a considerable gain in terms of miniaturization and switching rate. With the progress of nanotechnology, photochromic molecules will certainly play an important role in the coming years.

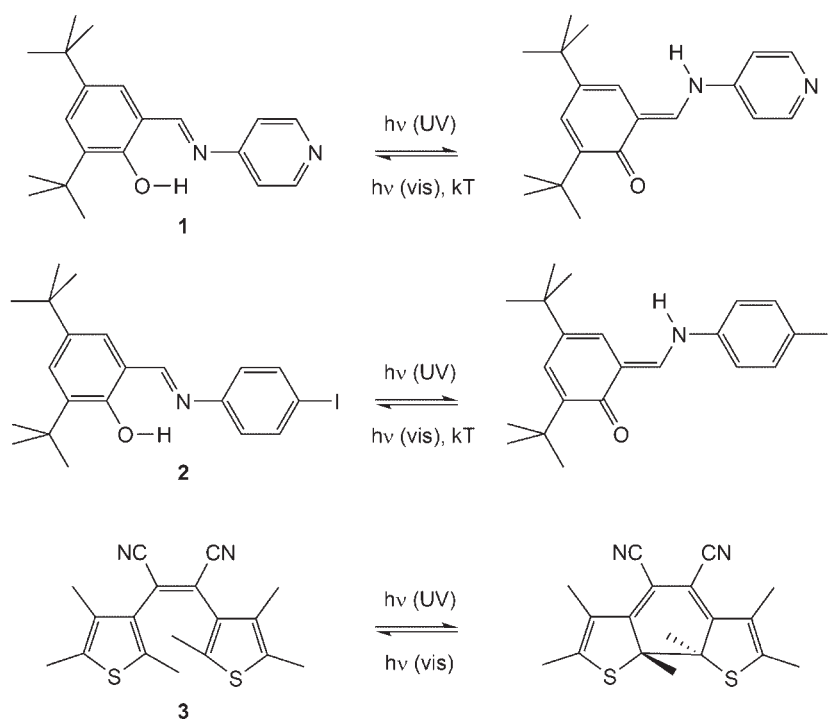
However, to progress toward such directions, (i) reliable techniques to produce nanoscale materials, and (ii) accurate methods to probe the material's state, are required. Nowadays, several techniques to fabricate nanocrystals and nanoscale thin layers exist, such as spin-coating, reprecipitation method,⁵ crystallization

combined with sol-gel method,⁶ laser ablation,⁷ and vapor deposition.⁸ Such techniques were exploited to fabricate nanoscale photochromic materials.⁹ Absorption measurement is the usual way of probing the photochromic system. However, one question arises: what is the minimal amount of material required to detect switching? Besides exploring the limits of absorption measurements, much research effort deals with more sensitive detection techniques to follow switching, which involve fluorescence,¹⁰ Raman scattering,¹¹ plasmon resonance.¹²

Our work belongs to this latter field. We fabricated nanocrystals and nanoscale thin layers of photochromes by vapor deposition on a glass substrate. Photo switching between the two states of the photochromes was investigated by absorbance measurements in the UV-visible range. The compounds we report in this paper are two anils (salicylidene-aniline and related compounds), *N*-(3,5-di-*tert*-butylsalicylidene)-4-aminopyridine (**1**),¹³ *N*-(3,5-di-*tert*-butylsalicylidene)-4-iodoaniline (**2**),¹⁴ and a diarylethene (**3**)¹⁵ (Scheme 1). The first two compounds, fully characterized (crystallographic structure and photochromic properties) in preceding works, were chosen because of their ability to yield photochromism in the bulk state with very limited thermal back reaction.^{13,14,16} Their nanostructures are very similar to bulk ones. Nanoscale thin layers of compound **3** are photoactive. This compound was also deposited on substrates

*Correspondence to: K. Nakatani, PPSM, ENS Cachan, CNRS, UniverSud, 61 av President Wilson, F-94230 Cachan, France.
E-mail: nakatani@ppsm.ens-cachan.fr

[†]Present Address: Materials Research Center, K.U. Leuven, Celestijnenlaan 200F, B-3001 Heverlee, Belgium.



Scheme 1. Photochromic reactions involving the investigated compounds **1**, **2**, and **3**

previously covered by gold nanoparticles, in order to investigate possible mutual influence between the photochrome's state and the plasmon.

EXPERIMENTAL

Sample preparation

Organic compounds. The syntheses of the first two compounds **1** and **2** have been described previously.^{13,14} Compound **3** is commercially available (B1536 obtained from TCI, Japan).

Preparation of the substrates. (i) Free glass substrate: Microscope glass substrates (Roth; 25 mm × 25 mm × 1 mm) were first carefully cleaned in a water/surfactant ultrasonic bath for 30 min, washed in distilled water, and sonicated in ethanol for 30 min. They were dried for 2 h at 80 °C and finally treated into a plasma-cleaner (Harrick PDC-002) to remove organic traces prior to deposition; (ii) Substrate covered by gold nanoparticles:¹⁷ Microscope glass substrates (Micro Slide Glass, Matsunami) were cleaned in a 1:1 solution of methanol and HCl for 30 min, washed extensively with distilled water, and dried overnight at 60 °C. The cleaned glass substrates were immersed in a 10% solution of 3-aminopropyltriethoxysilane (Nakalai Tesque) in anhydrous ethanol for 15 min, rinsed in ethanol with sonication, and dried at 120 °C for 3 h. Gold nanoparticles (mean diameter: 100 nm) were dispersed and fixed on the 3-aminopropyltriethoxysilane modified glass substrate by

adsorption from droplets of the colloidal solution (commercially available from British Biocell: EMGC100). The droplets were left on the substrate for about 10 min at room temperature and they were washed away with distilled water and dried with nitrogen.

Vapor deposition method. The deposition of thin films was carried out using a Leybold vacuum chamber. The pure organic powder obtained from the synthesis was introduced in the crucible (10 mm diameter by 25 mm long quartz cylinder). Various amounts of organic compounds were used: from several hundreds of milligrams for the ~10 μm thick films, down to a few milligrams for the nanoscale fabrication. The content of the crucible was heated to be pre-melted at atmospheric pressure, and let to reach room temperature before starting the deposition process. The crucible was heated in the furnace by means of tungsten filament at a rate of 10 °C min⁻¹ (from 25 to 120 °C). The temperature was controlled by a thermocouple. The deposition pressure (1–2 × 10⁻⁵ mbar) was fixed by the exhaust vacuum system. Organic molecules were condensed from the vapor phase onto a substrate positioned behind a mechanically operated shutter. Growth rate was monitored *in situ* by a piezoelectric quartz crystal microbalance.

Sample characterization

Atomic force microscopy (AFM). Topographic images and section profiles of the deposited samples

were performed using an Explorer AFM (Veeco) in ambient atmosphere. The scanner allowed 100 μm displacement in *X* and *Y* directions corresponding to the substrate plane, and up to 8 μm in *Z* direction. The characterization was obtained in tapping mode using a silicon non-contact probe (tip radius < 15 nm). The precision of the measurement is ± 2 nm in the *Z*-axis. Partially hidden substrates were used in order to compare the deposited material with blank areas (thickness determination and eventually dirt identification).

Optical profilometry. The macroscale films (thickness between 1 up to 10 μm) were characterized by an UBM Messtechnik GmbH optical profilometer with an accuracy of ± 500 nm in the *Z*-axis. The thickness was estimated by comparing the step height between the blank area of the substrate, protected during deposition, and the organic compound.

Absorption spectroscopy. Absorption spectra of thin films were performed on a double beam Varian Cary 5 spectrophotometer equipped with a home-built mechanical mounting which allows to control angular position with respect to the probe light.

Irradiation experiments. Photochromic reaction was induced *in situ* by a Hg/Xe lamp (Hamamatsu, LC6

Lightingcure, 150 W) equipped by filters of appropriate wavelengths.

RESULTS AND DISCUSSION

Salicylidene-aniline nanocrystals

Vapor deposition fabrication and AFM study.

Vapor deposition experiments were first performed with the two salicylidene-aniline compounds **1** and **2**. This general procedure (see Experimental Section) allowed a very thin and reproducible coverage of the whole substrate. Figure 1 displays the AFM images recorded on a vapor deposited sample of compound **1**. Two sub-populations of crystals are basically observed, some areas containing relatively large sized objects [Fig. 1(a)], and some others showing very small nanoparticles [Fig. 1(b)]. This behavior is especially underlined in Fig. 1(a). Most of the large crystals were identified as 'needle'-shaped [see A in Fig. 1(a)], which is in good agreement with the macroscopic crystal shape of this compound.¹³ Therefore, we can assume that the crystalline state is achieved by the deposition. The dimensions of all these larger crystals are typically comprised between the micro- and the nanoscale: as shown in the profile, most of them are 1–5 μm long along the needles axis and

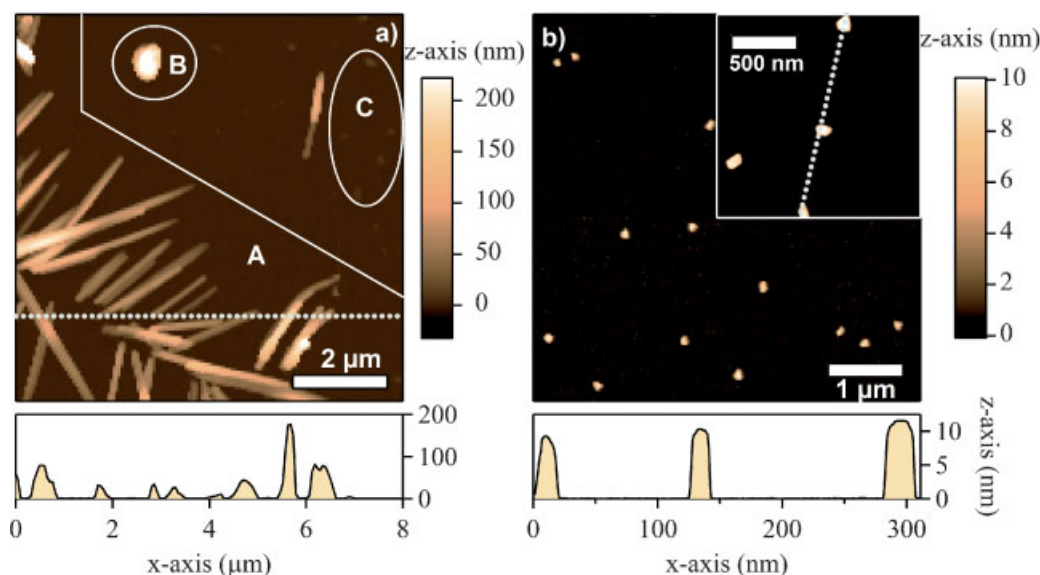


Figure 1. Atomic force microscopy of compound **1** deposited on a glass substrate. (a) The surface is covered by very heterogeneously size-distributed crystals. Two sub-populations of particles are observed: large objects such as 'needle'-shaped crystals (area A) or other shapes (area B), and small spot-like nanoparticles (dark area C). The horizontal profile shows the typical sizes of the observed crystals in region A; (b) Two images from areas similar to region C containing homogeneous dispersion of small nanoparticles were recorded with higher magnifications. Image profile allows accurate size determination along the *Z*-axis

have a 100–300 nm cross-section. Nevertheless, other kinds of shapes were also eventually observed [see B in Fig. 1(a)]. On the other hand, in some other locations, quite smaller crystals are also noticed. Such an example is shown in Fig. 1(a) (see region C). When zooming in such areas, a very homogeneous dispersion of nanoparticles was recorded as presented in Fig. 1(b). The sizes of such small spot-like objects were well-characterized by AFM. Image profiles [e.g., Fig. 1(b)] provide accurate measurements of their size in the Z-dimension (10–15 nm), and estimated values in the X/Y-dimensions (15–30 nm). The shape of these particles is mainly isotropic, with no evident favored direction of growth. All these observations were carefully checked to be reproducible.

Vapor deposited samples of compound **2** resulted in completely different outputs. With the same introduced amount as for compound **1** (a few milligrams), the surface of the glass substrate was covered by a distribution of medium-sized crystals. As illustrated in Fig. 2 (images and corresponding horizontal profile), the crystals sizes were characterized by AFM. Most of the crystals are in the 100–500 nm range (short axes) and 1–5 μm (long axis), with a parallelepiped shape. Once again, the very comparable basic shapes of these crystals with the macroscopic block crystals obtained by slow crystallization in solvent are a strong indication of the crystalline state of these deposited materials.¹⁴ Moreover, all the recorded AFM images (cf. Fig. 2 as an example) suggest that the long axis of the crystals is locally aligned along a

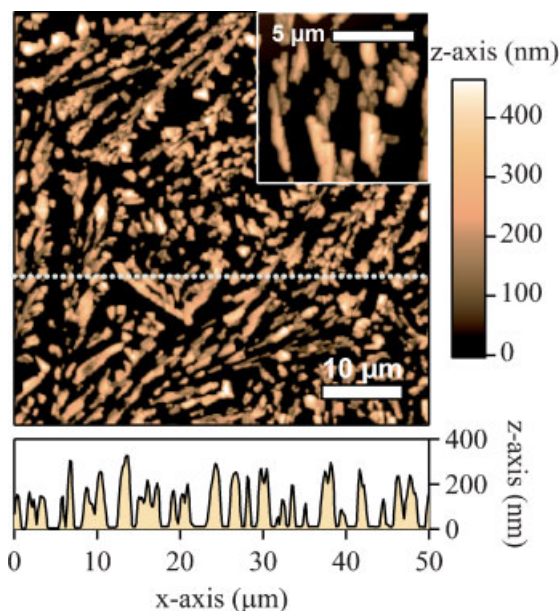


Figure 2. Atomic force microscopy of compound **2** deposited on a glass substrate. The surface is covered by a distribution of medium-sized crystals. The parallelepiped shape of the crystals is well-characterized by the AFM pictures at different magnifications and horizontal profile: sizes are comprised between 100–500 nm cross-section and 1–5 μm length

preferred direction, which could indicate the crystal growth direction.

Although all the experimental parameters were identical and well-controlled in the vacuum chamber (pressure, temperature increase rate, compound and substrate preparation), the morphology is different between compounds **1** and **2**. Despite their chemical structure similarity, the affinity of the molecules to the substrate, the melting point, and the crystalline structure are different for compounds **1** and **2**. Moreover, compound **2** shows a polymorphism.¹⁴ The obtained deposition depends on all these factors. Consequently the vapor depositions yield different crystal sizes and shapes.

Spectroscopic and photochromic studies. In order to investigate the photochromic behavior of the micro- and nanocrystals presented above and compare their properties to the macroscopic solid state level, we performed vapor deposited thin films with larger amounts of organic compounds. We used 70 mg (resp. 100 mg) and 170 mg (resp. 220 mg) of compound **1** (resp. **2**) to make thin films with thicknesses in the range of ~ 1 and $\sim 10 \mu\text{m}$, as determined by optical profilometry.

In ethanol solution, compounds **1** and **2** exhibit absorption bands in the 260–410 nm region, with maxima located at 289 and 362 nm for **1**, and 281, 315, and 368 nm for **2**. The corresponding keto photoisomers, obtained upon UV irradiation of the original enol forms, undergo a fast thermal back reaction in the microsecond range,¹⁸ which prevents any steady-state observation of the colored form of these compounds in solution. Nevertheless, in the solid state, the photoisomers are much more stable^{13,14} and photocoloration of the materials can be easily induced under continuous UV light. The differential absorption spectra of deposited samples of compound **1** upon UV irradiation with different thicknesses are shown in Fig. 3(a). The photocolored stationary state was reached within a few minutes of irradiation and displays an absorption band centered at 472 nm for the deposited solid film of the largest thickness, which is typical of salicylidene-anilines. Unsurprisingly, this steady-state red color was strongly attenuated, but still measurable, with the thinner film ($\sim 1 \mu\text{m}$ thick) and even more for the sample of **1** described in the AFM study above. These transformations are reversible. So the photochromic properties of compound **1** are successfully preserved at the micro- and nanoscales. However, this absorption band tends to be red-shifted when the thickness decreases [Fig. 3(a)]: the maximum is located at 518 nm for the two samples of the smaller sizes. Such a spectral red-shift could be tentatively attributed to stronger interface interactions with the substrate, which could induce a change of the conformation of the keto form. Fig. 3(b) displays the corresponding differential absorption spectra of compound **2**. In this case, no red-shift was detected. Unfortunately, no direct evidence of the photochromic properties was observed for the nanoscaled depositions,

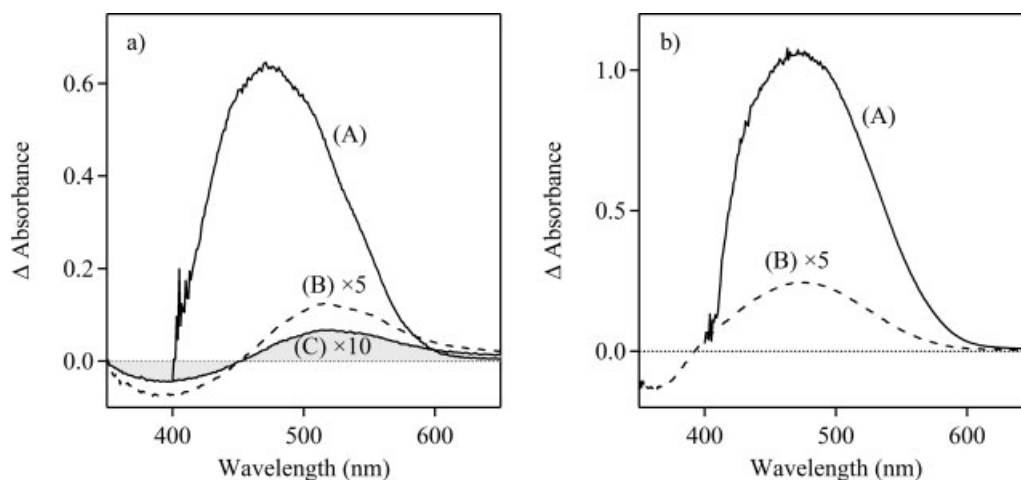


Figure 3. Differential absorption spectra obtained from vapor deposited photochromic samples of compounds **1** (a) and **2** (b), before and after continuous UV irradiation. Irradiation wavelength was set to 405 nm (A–B) or 365 nm (C). (A) and (B): film thickness ~ 10 and ~ 1 μm , respectively. (C): deposited micro- and nanocrystals

due to unfavorable signal-to-noise, scattering, and waveguide effects when recording the absorption spectra. Nevertheless, a very slight and reversible change of the absorption spectra occurs and is a good indication that compound **2** is still photoactive in nanoscale crystals.

Nanometer-scale thin layers

Deposition on glass substrate. The same experimental procedure as for compounds **1** and **2** was used for the diarylethene compound **3**, in order to make very thin vapor depositions of photochromic materials on a glass surface. Since the result strongly depends on the procedure, careful preparation of the sample is essential. On one hand, when compound **3** was directly sublimated without further pre-melting in the crucible, the deposition produced large and aggregated crystals dispersed on the surface [Fig. 4, inset]. The resulting glass plate is typically opaque. Section profile A in Fig. 4 points out the heterogeneously distributed sizes of the deposited materials, which range from 100 nm up to about 1 μm . On the other hand, when the organic precursor was properly pre-melted and cooled down to room temperature before vapor deposition, a very homogeneous thin film was successfully obtained, as characterized by the main AFM image in Fig. 4. The thickness of such a film was accurately measured by AFM to be 65 ± 5 nm on a quite large area (several 10^3 – 10^4 μm^2 areas have been scanned). In this case, the transparency and the flatness on a long-range of the thin nanometer-scaled layer denote the amorphous state of the organic deposition. The photochromic properties of the thin layer were then examined and absorption spectra were recorded before and after light irradiation at 405 nm [Fig. 5(a) and (b)]. The inset in Fig. 5 presents the spectral change upon UV

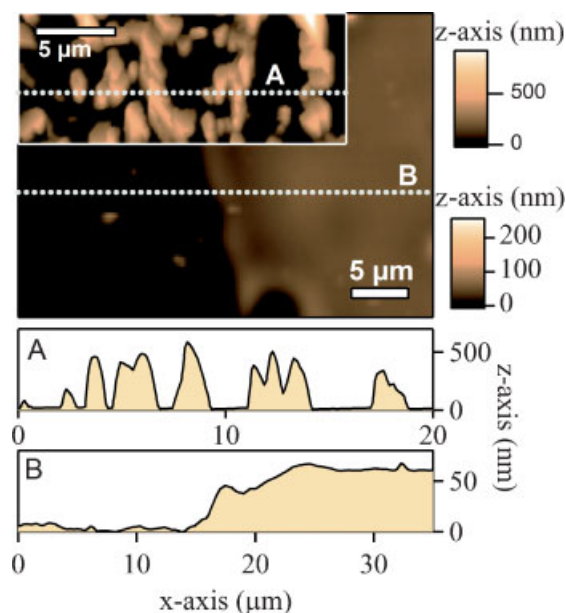


Figure 4. Atomic force microscopy of a thin layer of compound **3** vapor deposited on simply cleaned glass substrate. Inset: aggregated crystals obtained when the organic precursor was not pre-melted in the crucible. Section profiles (A) and (B) present the typical sizes of the surface depositing

irradiation (curve h). This differential spectrum has the same shape as that of chloroform solution or that of a thick sample obtained from melt between two cover glasses (average thickness ~ 10 μm deduced from weight, area, and estimated density; curve f). In spite of the low intensity of the induced pink color, the absorption change is still detectable by conventional spectroscopy and perfectly reversible when irradiated at 532 nm. As a conclusion, we succeeded in producing a vapor deposited organic nanolayer (~ 65 nm) with photochromic properties.

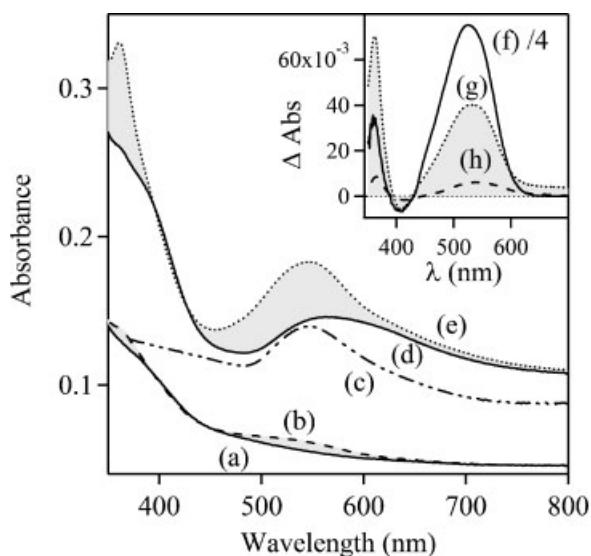


Figure 5. Absorption spectra of amorphous nanometerized thin films. Compound **3** before (a) and after (b) UV irradiation. Hybrid nanolayers before (d) and after (e) UV irradiation. Inset shows differential spectra: (h) = (b) – (a) and (g) = (e) – (d). Absorption spectrum of gold nanoparticles deposited on a modified glass substrate (c), and differential spectrum of a $\sim 10\ \mu\text{m}$ -thick film prepared by the melting technique (h) are given for comparison. UV irradiation: 1 min at 405 nm

Deposition on substrate covered by gold nanoparticles. Figure 6 presents the AFM image of compound **3** deposited as a thin amorphous layer on a gold-covered substrate. The thickness of the hybrid thin film ($\sim 100\ \text{nm}$) was adjusted to the gold particles

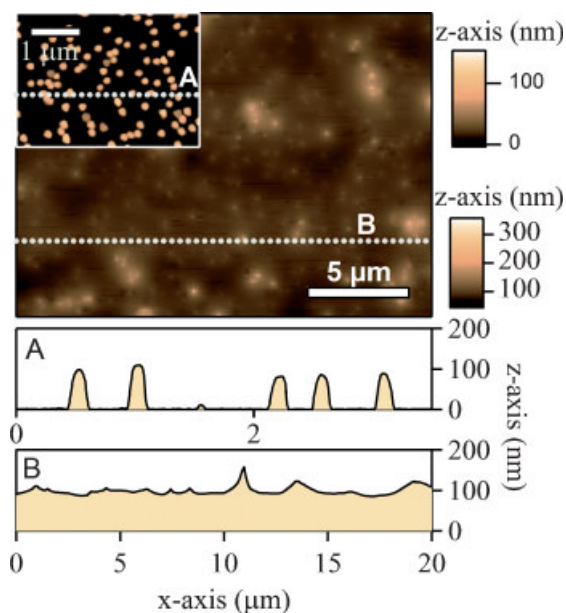


Figure 6. Atomic force microscopy of a modified glass substrate bearing gold nanoparticles covered by a nanolayer of compound **3**. Inset: gold nanoparticles distributed on the substrate before vapor deposition of **3**. Section profiles (A) and (B) display the sample topography before and after the deposition

diameter [section profiles in Fig. 6]. Therefore, the vapor deposition was sufficient to cover the whole metallic assembly and yielded a rather homogeneous hybrid nanolayer. The characteristic absorption band of compound **3** appears in the UV region [below 430 nm, curves d and e in Fig. 5]. The effect of the organic material on the local surface plasmon resonance of the gold nanoparticles is also mentioned in Fig. 5. This band is enlarged and its maximum is red-shifted up to 565 nm after deposition of compound **3**. This is interpreted within the context of refraction index change of the surrounding material. Actually, the organic layer induces an increase of the medium's index, leading to a red-shift of the plasmon band.¹⁹ The absorption spectrum of the hybrid nanolayer upon irradiation at 405 nm is displayed in Fig. 5(e). The shape of the corresponding differential spectrum shown in Fig. 5(g) is comparable to the photochromic thin films without gold nanoparticles [Fig. 5 (f, h)]. We can deduce that the absorption change upon UV irradiation is essentially due to the colored state of compound **3**. Even though we could not observe any change of the plasmon resonance band upon UV irradiation, the color change was observed to be higher in the case of the hybrid nanolayer [Fig. 5(g)] compared to the simple deposition of compound **3** [Fig. 5(h)]. At the present stage, several hypotheses are conceivable and we cannot fully explain the exact mechanism of the phenomenon. Since we irradiated in the UV region, which is far from the local surface plasmon resonance peak (580 nm) of the gold nanoparticles, electromagnetic enhancement effects due to the plasmon resonance are not expected. Further experiments are in progress in order to distinguish between plasmon enhancement effects, quenching of excited states by the gold nanoparticle, and modification of the photochromic quantum yields near the metal surface.

CONCLUSION

Photochromic nanoscale materials were prepared by vapor deposition method. By tuning the experimental conditions, we obtained different nanoscale structures. We demonstrated that photochromism is preserved in hybrid nanomaterials, and this stimulates further investigations on the effects of nanoscale interactions.

Acknowledgements

SAKURA program (JSPS-EGIDE) and Japan-France Doctoral College program are acknowledged for supporting this collaboration.

REFERENCES

1. Marckwald WZ. *Zeitschr. Phys Chem.* 1899; **30**: 140–145.
2. Crano JC, Guglielmetti RJ. (eds). *Organic Photochromic and Thermochromic Compounds*. Plenum: New York, 1998; Special

- Issue on Photochromism: Memories and Switches. *Chem. Rev.* 2000; **100**: 1683–1890.
3. (a) Higgins S. *Chim. Oggi—Chem. Today* 2003; **21**: 63–67; (b) Winder R. *Chem. Ind.* 2006; **12**: 20–21.
 4. (a) Kawata S, Kawata Y. *Chem. Rev.* 2000; **100**: 1777–1788; (b) Irie M, Kobatake S, Horichi M, *Science* 2001; **291**: 1769–1772; (c) Feringa BL. (ed.). *Molecular Switches*. Wiley-VCH: Weinheim, 2003.
 5. (a) Kasai H, Oikawa H, Okada S, Nakanishi H. *Bull. Chem. Soc. Jpn.* 1998; **71**: 2597–2601; (b) Fu HB, Yao JN. *J. Am. Chem. Soc.* 2001; **123**: 1434–1439.
 6. Ibanez A, Maximov S, Guiu A, Chaillout C, Baldeck PL. *Adv. Mater.* 1998; **10**: 1540–1543.
 7. Tamaki Y, Asahi T, Masuhara H. *J. Phys. Chem. B* 2002; **106**: 2135–2139.
 8. (a) Shtein M, Gossenberger HF, Benziger JB, Forrest SR. *J. Appl. Phys.* 2001; **89**: 1470–1476; (b) Seko T, Ogura K, Kawakami Y, Sugino H, Toyotama H, Tanaka J. *Chem. Phys. Lett.* 1998; **291**: 438–444.
 9. (a) Kobatake S, Kuratani H. *Chem. Lett.* 2006; **35**: 628–629; (b) Sun F, Zhang FS, Zhao FQ, Zhou XH, Pu SZ. *Chem. Phys. Lett.* 2003; **380**: 206–212; (c) Spagnoli S, Block D, Botzung-Appert E, Colombier I, Baldeck PL, Ibanez A, Corval A. *J. Phys. Chem. B* 2005; **109**: 8587–8591; (d) Ishow E, Bellaiche C, Bouteiller L, Nakatani K, Delaire JA. *J. Am. Chem. Soc.* 2003; **125**: 15744–15745; (e) Shirota Y. *J. Mater. Chem.* 2000; **10**: 1–25; (f) Chauvin J, Kawai T, Irie M. *Jpn. J. Appl. Phys.* 2001; **40**: 2518–2522.
 10. Irie M, Fukaminato T, Sasaki T, Tamai N, Kawai T. *Nature* 2002; **420**: 759–760.
 11. Maurel F, Troung SL, Bertigny JP, Dubest R, Levi G, Aubard J, Delbaere S, Vermeersch G. *Mol. Cryst. Liq. Cryst.* 2005; **430**: 235–241.
 12. (a) Dulic D, van der Molen SJ, Kudernac T, Jonkman HT, de Jong JJD, Bowden TN, van Esch J, Feringa BL, va Wees BJ. *Phys. Rev. Lett.* 2003; **91**: art. no 207402; 2074021–2074024; (b) Kudernac T, van der Molen SJ, van Wees BJ, Feringa BL. *Chem. Commun.* **2006**: 3597–3599; (c) He J, Chem F, Liddell PA, Andreasson J, Straight SD, Gust D, Moore TA, Moore AL, Li J, Sankey OF, Lindsay SM. *Nanotechnol.* 2005; **16**: 695–702.
 13. Sliwa M, Létard S, Malfant I, Nierlich M, Lacroix PG, Asahi T, Masuhara H, Yu P, Nakatani K. *Chem. Mater.* 2005; **17**: 4727–4735.
 14. Spangenberg A, Sliwa M, Métivier R, Dagnelie R, Nakatani K, Pansu R, Malfant I. *J. Phys. Org. Chem.* **2007**: (in press).
 15. Irie M, Mohri M. *J. Org. Chem.* 1988; **53**: 803–808.
 16. (a) Hadjoudis E, Mavridis IM. *Chem. Soc. Rev.* 2004; **33**: 579–588; (b) Hadjoudis E. In *Photochromism: Molecules and Systems*, Dürr H, Bouas-Laurent H (eds). Elsevier: Amsterdam, the Netherlands, 1990: 685–712; (c) Amimoto K, Kawato T. *J. Photochem. Photobiol. C* 2005; **6**: 207–226.
 17. Nath N, Chilkoti A. *Anal. Chem.* 2002; **74**: 504–509.
 18. (a) Nakagaki R, Kobayashi T, Nakamura J, Nagakura S. *Bull. Chem. Soc. Jpn.* 1977; **50**: 1909–1912; (b) Wettermark G, Dogliotti L. *J. Chem. Phys.* 1964; **40**: 1486–1487.
 19. (a) Bohren CF, Huffman DR. *Absorption and Scattering of Light by Small Particles*. Wiley: New York, 1983; (b) Itoh T, Asahi T, Masuhara H. *Jpn. J. Appl. Phys.* 2002; **41**: L76.